

When Alignment Fails: Multimodal Adversarial Attacks on Vision-Language-Action Models

Yuping Yan¹, Yuhan Xie¹, Yixin Zhang², Lingjuan Lyu³, Handing Wang⁴, Yaochu Jin^{1†}

¹TGAI Lab, School of Engineering, Westlake University

²Pennsylvania State University ³Sony Research, Sony ⁴Xidian University

{yanyuping, xieyuhan, jinyaochu}@westlake.edu.cn

[†]Corresponding author

Abstract

Vision-Language-Action models (VLAs) have recently demonstrated remarkable progress in embodied environments, enabling robots to perceive, reason, and act through unified multimodal understanding. Despite their impressive capabilities, the adversarial robustness of these systems remains largely unexplored, especially under realistic multimodal and black-box conditions. Existing studies mainly focus on single-modality perturbations and overlook the cross-modal misalignment that fundamentally affects embodied reasoning and decision-making. In this paper, we introduce VLA-Fool, a comprehensive study of multimodal adversarial robustness in embodied VLA models under both white-box and black-box settings. VLA-Fool unifies three levels of multimodal adversarial attacks: (1) textual perturbations through gradient-based and prompt-based manipulations, (2) visual perturbations via patch and noise distortions, and (3) cross-modal misalignment attacks that intentionally disrupt the semantic correspondence between perception and instruction. We further incorporate a VLA-aware semantic space into linguistic prompts, developing the first automatically crafted and semantically guided prompting framework. Experiments on the LIBERO benchmark using a fine-tuned OpenVLA model reveal that even minor multimodal perturbations can cause significant behavioral deviations, demonstrating the fragility of embodied multimodal alignment.

1. Introduction

Vision-Language-Action (VLA) models represent a new frontier in robotic manipulation, bridging perception, reasoning, and control [11, 34]. By integrating large language models (LLMs) and vision-language models (VLMs), these systems enable robots that can see, understand, and act, transforming natural instructions into fine-grained, context-

aware actions [20, 31]. Recent deployments across manufacturing [9], healthcare [14], and service robotics [20] have further demonstrated the transformative potential of VLA-driven systems, highlighting their ability to generalize across diverse embodied environments.

However, despite this rapid progress, current VLA models remain far from reliable in real-world settings [16, 35]. Their robustness, cross-modal alignment, and behavioral consistency are still major challenges. When deployed outside controlled environments, VLA systems are exposed to subtle prompt manipulations, unpredictable visual variations, and unstable physical conditions [5]. These factors can easily mislead the model’s perception or reasoning, triggering unintended or unsafe actions, often without immediate detection.

Existing studies have examined the robustness of VLA-based robotic systems through various attack modalities, including prompt injection in textual inputs [10], adversarial patch generation that creates localized perturbations via gradient-based optimization [29], and physical perturbations such as blurring, Gaussian noise, brightness and darkness variations, object pose transformations, and illumination changes [5, 16, 32]. However, most of these efforts overlook the attacker’s threat model, often assuming white-box access and ignoring more realistic black-box attack scenarios commonly encountered in the physical world. Furthermore, current research typically focuses on single-modality attacks, neglecting the intricate cross-modal interactions between vision and language that define VLA systems. This leaves open a crucial question: *how do multimodal perturbations affect the stability, alignment, and decision-making of embodied VLA agents?*

To address these challenges, we introduce VLA-Fool, a comprehensive adversarial evaluation suite for embodied VLA models under realistic multimodal, white-box and black-box threat settings. Unlike prior efforts that target either visual or textual channels in isolation, VLA-Fool

jointly attacks language, vision, and cross-modal alignment, enabling the first systematic assessment of robustness across the entire perception-language-action pipeline. The main contributions of this work are as follows:

- We propose VLA-Fool, a comprehensive framework for generating and evaluating multimodal adversarial attacks under both white-box and black-box settings. Our framework encompasses (i) textual perturbations through semantically guided gradient-based and prompt manipulation strategies, (ii) visual perturbations via patch-based and noise-based distortions, and (iii) cross-modal misalignment attacks that deliberately disrupt the semantic correspondence between perception and instruction, providing a holistic assessment of embodied VLA robustness.
- By extending the Greedy Coordinate Gradient (GCG) approach into a VLA-aware semantic space, we introduce the first automatically crafted, semantically guided prompting framework tailored for VLA adversarial attacks, including four linguistically rich misalignment modes, referential ambiguity, attribute weakening, scope blurring, and negation confusion.
- Through extensive experiments, we reveal the fragility of state-of-the-art VLA models when exposed to multimodal perturbations, with failure rates exceeding 60% across all variation categories, and up to 100% failure in long horizon tasks, offering valuable insights and benchmarks for developing more robust and trustworthy embodied agents.

2. Related Work

2.1. VLA models for embodiments

Recent progress in VLA models has advanced embodied intelligence by unifying perception, reasoning, and control [34]. Supported by large-scale multimodal datasets and realistic simulators, existing methods can be broadly categorized into autoregressive [13, 19], diffusion-based [6], and hybrid integration paradigms. Autoregressive models treat action generation as a temporally dependent process, decoding motion trajectories or control tokens step by step from multimodal inputs [30]. Representative examples include RT-1/RT-2 [4, 36], Octo [28], OpenVLA [11], and SpatialVLA [24]. Diffusion-based approaches shift robotic action generation from deterministic regression to probabilistic generative modeling, allowing policies to better capture uncertainty and diverse action distributions [23]. By introducing geometry-aware representations and self-supervised objectives, models such as ForceVLA [33], RDT-1B [18], π_0 [3], TinyVLA [31], and SmolVLA [27] achieve stronger multi-task generalization, few-shot adaptation, and language-conditioned control in complex embodied environments. Hybrid frameworks integrate the long-

horizon reasoning capability of autoregressive models with the fine-grained generative flexibility of diffusion architectures. For instance, HybridVLA [17] unifies continuous trajectory generation and token-level reasoning within a single large-scale (7B-parameter) model, marking a step toward more scalable and unified multimodal embodiment.

2.2. Adversarial attacks for VLA models

An adversarial attack refers to deliberate manipulation of a model’s input to induce incorrect or unintended outputs [8]. Such attacks can be applied to both text and visual inputs.

2.2.1. Textual adversarial attack

Textual adversarial attacks manipulate linguistic inputs to induce incorrect or unsafe behaviors in multimodal and embodied systems. Among existing approaches, the Greedy Coordinate Gradient (GCG) algorithm [37] is a representative white-box method that iteratively optimizes prompt tokens to maximize a model’s response deviation. Building on this, Jones et al. [10] introduces the first VLA-oriented textual attack based on GCG and later extends it to a black-box setting through a transfer-based strategy, where optimized prompts crafted on a source model can be effectively transferred to one or more target models. Despite these advances, most text-based attacks still focus on LLM-driven embodied agents rather than fully integrated VLA systems. For example, BadRobot [35] targets unsafe or irrational behaviors in language-centric robots, while the multimodal misalignment vulnerabilities of VLA architectures remain largely underexplored.

2.2.2. Visual adversarial attack

Visual adversarial attacks aim to manipulate the perception of an embodied model by injecting crafted image perturbations that lead to erroneous actions. Wang et al. [29] conducted the first systematic analysis of VLA robustness, proposing the Untargeted Action Discrepancy Attack and the Untargeted Position-Aware Attack. Both are white-box patch-based methods that directly exploit gradient information to make OpenVLA generate deviated trajectories on a 7-DoF robotic arm, but they rely on full model access and simulation control. The subsequent Embedding Disruption Patch Attack [32] relaxed these constraints by requiring access only to encoder parameters, achieving more transferable and architecture-agnostic attacks. Beyond synthetic perturbations, several studies have investigated real-world physical vulnerabilities of embodied VLAs. Cheng et al. [5] demonstrated that noise, brightness variations, and visual prompt interference can significantly reduce the manipulation accuracy. Similarly, Liu et al. [16] assessed VLA performance under black-box conditions, considering object 3D transformations, illumination variations, and adversarial patches. Together, these works reveal that current VLA systems remain highly sensitive to visual perturbations and

environmental changes, underscoring the need for deeper robustness analysis under multimodal and physical-world settings.

3. Threat model and problem formulation

Given a visual observation I and a natural-language instruction T , a VLA model produces an executable action vector A :

$$A = M(I, T) = f(\mathcal{E}_v(I), \mathcal{E}_t(T)) \quad (1)$$

where $\mathcal{E}_v(\cdot)$ and $\mathcal{E}_t(\cdot)$ are the vision and language encoders, respectively, and $f(\cdot)$ denotes the multimodal backbone followed by an action de-tokenizer that outputs motor control parameters such as translation Δx , rotation $\Delta\theta$, and gripper state $\Delta grip$.

3.1. Threat model

Depending on capabilities and goals, the threat model can be characterized into two levels of model access:

- **White-box:** the adversary has full knowledge of the VLA stack: model architecture, weights, intermediate representations, and gradients. This enables gradient-based optimization through the vision encoder, the language encoder, and the action head. White-box access is the strongest digital threat and is used to evaluate the worst-case vulnerabilities.
- **Black-box:** the adversary only observes model outputs, including the discrete actions, continuous trajectories, or scalar scores, and has no internal gradient or embedding access. Black-box attacks represent the most practical, efficient, and realistic threat model for deployed VLA systems.

3.2. Attack surface and objective

The adversary aims to craft perturbed multimodal inputs (I_{adv}, T_{adv}) that mislead the victim model M into producing any incorrect action A_{adv} . The general attack pipeline is:

$$A_{adv} = M(I_{adv}, T_{adv}), \quad (I_{adv}, T_{adv}) = \text{atk}(I, T; \delta_v, \delta_t) \quad (2)$$

where δ_v and δ_t denote perturbations applied to visual and textual modalities, and $\text{atk}(\cdot)$ represents the attack generation function. Attack surfaces include (i) textual perturbations (prompt injections, token edits), (ii) visual perturbations (patch-based and noise-based), and (iii) cross-modal misalignment (semantic disruption between $\mathcal{E}_v(I)$ and $\mathcal{E}_t(T)$).

The attack optimization objective can be formulated as:

$$\min_{\delta_v, \delta_t} \mathcal{L}_{\text{attack}}(M(I + \delta_v, T + \delta_t), A) \quad (3)$$

4. VLA-Fool: A multimodal adversarial attack suite

To comprehensively evaluate the robustness of VLA models, we propose VLA-Fool, a unified attack suite that systematically encompasses textual, visual, and cross-modal misalignment adversarial attacks, as presented in Figure 1.

4.1. Textual attacks

Textual attacks seek to generate an adversarial instruction T_{adv} that forces an embodied VLA model $M(I, T)$ to produce an undesired action A_{adv} , thereby breaking the vision-language grounding. To comprehensively evaluate linguistic robustness, we implement two classes of textual attacks: (i) Semantically Greedy Coordinate Gradient (SGCG) attack (white-box), and (ii) prompt manipulation attacks (black-box).

4.1.1. SGCG (white-box)

Recognizing that robotic VLA instructions critically rely on spatial references and entity descriptions, SGCG extends the GCG framework to strategically perturb these task-specific linguistic elements. Its objective is to generate a set of K independent adversarial instructions, $\mathcal{T}_{adv} = \{T_{adv}^{(1)}, \dots, T_{adv}^{(K)}\}$, from a single initial instruction T . Each $T_{adv}^{(k)}$ is optimized to maximize the attack loss $\mathcal{L}_{\text{attack}}$ while focusing on a distinct semantic perturbation strategy k .

For this study, we set $K = 4$ to enable a fine-grained evaluation across four types of semantically guided perturbations: referential ambiguity, attribute weakening or substitution, scope/quantifier blurring, and negation-based confusion. The definitions are as follows:

- **Referential ambiguity (SGCG 1).** This perturbation weakens explicit referential cues, targeting the model’s object-grounding stage. Specifically, tokens denoting concrete entities are replaced with pronouns or generic nouns, e.g., “it,” “that one,” “the object,” or “the item”.
- **Attribute weakening or substitution (SGCG 2).** In this strategy, discriminative attributes essential for fine-grained visual matching are altered or removed. The candidate set includes alternative attribute tokens across color (e.g., red replaced with blue), size (e.g., large replaced with small), and material (e.g., steel replaced with plastic).
- **Scope/quantifier blurring (SGCG 3).** This category perturbs spatial reasoning by relaxing quantifiers or spatial descriptors. The candidate set includes replacements such as substituting “left-most” with “on the left”, “between” with “near”, or “all” with “some”.
- **Negation/comparative confusion (SGCG 4).** This perturbation introduces mild negation or comparative phrasing that alters the logical inference process within the language-policy interface. Candidate tokens include negators such as not, do not, and never, as well as comparative

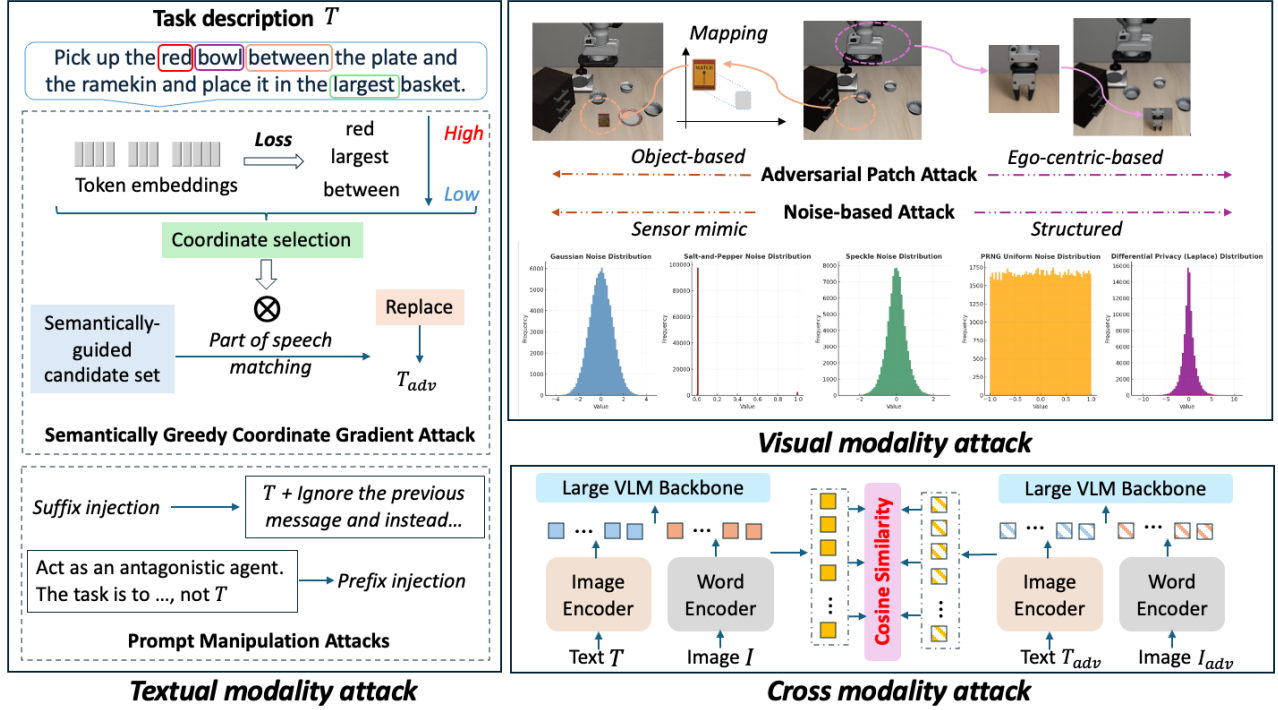


Figure 1. Overview of the VLA-Fool framework for multimodal adversarial attacks. The framework consists of three complementary modules targeting distinct modalities: (a) Textual modality attack, (b) Visual modality attack, and (c) Cross modality attack.

substitutions such as replacing “smallest” with “second smallest” or “largest” with “not the largest”.

With these strategies, SGCG executes K parallel GCG optimization processes, independently optimizing each $T_{adv}^{(k)}$. This parallel design ensures that each adversarial instruction targets its designated semantic vulnerability. The algorithm proceeds as follows:

- Step 1: Independent gradient focusing and coordinate selection. At iteration t , we identify the most sensitive token position i^* by computing the gradient of the attack loss $\mathcal{L}_{\text{attack}}$ with respect to token embeddings. We select the coordinate with the maximal gradient norm:

$$i^* = \arg \max_i |\nabla_{e_i} \mathcal{L}_{\text{attack}}(M(I, T))| \quad (4)$$

- Step 2: Construct semantically-guided candidate set. For the selected position i^* and semantic class k , we construct a focused candidate pool:

$$\mathcal{C}_{VLA}^k(T) = \mathcal{C}_G \cup \mathcal{C}_L^k(T) \quad (5)$$

where \mathcal{C}_G contains general gradient-sensitive proposals (embedding nearest neighbors, masked-LM suggestions) and $\mathcal{C}_L^k(T)$ contains class-specific substitutes (e.g., pronouns for referential ambiguity, color/size attributes for attribute weakening, spatial prepositions for position

fuzzing, and templates for negation/quantifiers). This design guarantees that at the most influential position i^* , we have access to the most destructive, category-specific semantic substitutions with the five categories.

- Step 3: Greedy substitution and update. At the selected coordinate i^* , each parallel task k independently searches for the optimal replacement token c^* from $\mathcal{C}_{VLA}^k T$. We enforce a Part-of-Speech matching [7] constraint $P(c) = P(w_{i^*})$ to maintain the syntactic fluency of the generated instruction T_{adv} :

$$c^* = \arg \max_{\substack{c \in \mathcal{C}^{(k)} \\ P(c)=P(w_{i^*})}} \mathcal{L}_{\text{attack}}(M(I, \mathcal{R}(T, i^*, c))) \quad (6)$$

where \mathcal{R} means the replacement function. Finally, each parallel task independently updates its adversarial instruction $T_{adv}^{(k)}$.

4.1.2. Prompt manipulations (black-box).

Inspired by recent findings in LLM adversarial security, we evaluate simple, black-box prompt injection attacks, which can be categorized into suffix injection and prefix injection. These attacks require no access to the model’s parameters or gradients, serving as a vital baseline to assess the VLA model’s vulnerability to basic adversarial framing and contextual shifts.

- **Suffix injection (Context overriding).** We investigate appending adversarial strings to the end of the correct instruction T . This strategy exploits the VLA model’s reliance on the final tokens in the sequence for action generation. Specifically, we implement two highly disruptive variants:

- **Context reset:** Appending a directive such as “ignore the previous message and instead ...” which attempts to completely override the initial instruction T , forcing the model to re-interpret its goal based only on the subsequent text.

- **Tokenization bypass (random code):** Appending non-standard, randomized strings or “code blocks” (e.g., `<script> print 100101; ignore all`), designed to disrupt the tokenizer’s stability and inject confusing, high-entropy tokens into the textual embedding sequence.

- **Prefix injection (Initial misdirection).** We evaluate prepending adversarial directives or confounding contextual information to the beginning of T . This attack aims to establish an incorrect initial context or force role misdirection before the core instruction is processed, potentially confusing the transformer’s self-attention mechanism. An example directive is prepending “Act as an antagonistic agent. The primary objective is to overturn the table, not T .”

4.2. Visual attacks

Visual attacks perturb the visual observation I to mislead a VLA model $M(I, T)$ so that it produces adversarial actions A_{adv} . In VLA-Fool, we implement two complementary visual attack families: (i) localized patch-based attack (white-box) and (ii) noise-based perturbation attacks (black-box).

4.2.1. Localized patch-based attack (white-box).

This attack is designed to generate semantically rich patches that are visually plausible within the robotic scene context. It utilizes full access to the model’s gradients to directly optimize the patch content δ_p . The adversarial image I_{adv} is generated by applying a placement operator $P(\cdot)$ that inserts the patch δ_p into a fixed region Ω of the image I :

$$I_{adv} = I + P(\delta_p) \quad (7)$$

We consider two distinct patch application strategies, testing different aspects of VLA robustness:

- **Environmental object patches:** Patches that mimic small, common objects naturally occurring in the task scene (e.g., small blocks or tools). These test the model’s ability to selectively ignore irrelevant scene distractors.

- **Robot-mounted patches:** Patches physically attached to the robot’s end effector or arm, inspired by prior work on object detection and tracking failures [10]. These test the

model’s reliance on the ego-centric view of the manipulation process.

The optimization objective is to maximize the deviation between the VLA’s correct action A and the adversarial action $M(I_{adv}, T)$. We use a direct L_2 distance maximization for the continuous action space:

$$\max_{\delta_p} \mathcal{L}_{\text{attack}}(I_{adv}) = \|A - M(I_{adv}, T)\|_2^2 \quad (8)$$

The optimization process utilizes gradient ascent on the parameterized patch content δ_p .

4.2.2. Noise-based perturbation attack (black-box).

To evaluate the model’s sensitivity to realistic imaging corruptions that mimic sensor noise, transmission errors, or environmental degradation under black-box constraints, we inject a variety of noise and texture perturbations. These attacks serve as a strong baseline, requiring no model gradients. We categorize the tested corruptions as follows:

- **A priori noise family** including standard sensor-mimicking noise models such as Gaussian [21], Salt-and-Pepper [1], and Speckle noise [25].

- **Structured and randomized corruptions** including uniform noise [2], pseudo-random (PRNG) patterns [12] designed to confuse high-level features, and differential-privacy style randomization [22] which tests resilience to random data obfuscation.

We measure the drop in success rate across various severity levels for each noise family to quantify the VLA model’s robustness against real-world degradation.

4.3. Cross-modal misalignment attack

Cross-modal misalignment attacks do not merely perturb one modality in isolation, instead, they seek an optimal adversarial pair (δ_v, δ_t) that maximizes the loss:

$$\max_{\delta_v, \delta_t} \mathcal{L}_{\text{mis}}(I + \delta_v, T + \delta_t) \quad (9)$$

Let $\mathcal{E}_v(\cdot)$ and $\mathcal{E}_t(\cdot)$ be the model’s visual and textual encoders, respectively. The *Cross-Modal Misalignment Loss* (\mathcal{L}_{mis}) combines two terms: a representational misalignment term and an action deviation term.

We use \mathbf{p}_i and \mathbf{w}_j to denote the i -th visual patch embedding and j -th language token embedding of the clean pair, and \mathbf{p}'_i and \mathbf{w}'_j for the perturbed pair. N and M are the number of visual patches and language tokens.

$$\mathcal{L}_{\text{mis}} = \frac{1}{N \times M} \sum_{i=1}^N \sum_{j=1}^M |\cos(\mathbf{p}_i, \mathbf{w}_j) - \cos(\mathbf{p}'_i, \mathbf{w}'_j)| \quad (10)$$

Here, $\cos(\cdot, \cdot)$ is the cosine similarity function. By maximizing this loss, the optimization process actively maximizes the difference between the clean, patch-to-token

Attack Type			LIBERO				Average
			Spatial	Object	Goal	Long	
Textual	◇ Gradient-Based	GCG	73.81%	80.00%	88.10%	75.00%	79.23%
		SGCG 1	50.00%	83.33%	88.10%	75.00%	74.11%
		SGCG 2	33.33%	83.33%	54.76%	54.17%	56.40
		SGCG 3	40.48%	43.33%	36.71%	50.00%	39.88%
		SGCG 4	36.71%	46.67%	45.24%	75.00%	52.32%
	♣ Prompt-Based	Suffix 1	69.05%	53.33%	88.10%	75.00%	71.31%
		Suffix 2	69.05%	76.67%	100%	83.33%	82.26%
		Prefix	23.81%	63.33%	33.33%	41.47%	40.54%
	Visual	◇ Patch-Based	Object	64.00%	66.80%	77.80%	94.6%
Arm			100%	100%	100%	100%	100%
♣ Noise-Based		Gaussian Noise ($\sigma = 30$)	21.43%	86.67%	19.05%	66.67%	48.46%
		Salt Pepper Noise ($\sigma = 0.02$)	76.19%	96.67%	83.33%	83.30%	84.87%
		Speckle Noise ($a = 0.3$)	33.33%	87.00%	45.24%	50.00%	53.81%
		Uniform Noise ($\sigma = 250$)	28.57%	90.00%	21.43%	66.67%	51.67%
		PRNG Noise ($\sigma = 30$)	23.81%	97.00%	23.81%	70.83%	53.78%
		DP ($\epsilon = 0.02$)	14.29%	66.67%	85.71%	33.33%	50.00%
Cross Misalignment	Spatial	-	92.86%	100%	100%	97.62%	
	Object	100%	-	96.67%	90.00%	95.56%	
	Goal	90.00%	100%	-	100%	96.67%	
	Long	100%	100%	100%	-	100%	

Table 1. Failure Rate (higher is worse) of VLA-Fool across textual, visual, and cross-modal attacks on the LIBERO benchmark. ◇ represents the white-box attacks, and ♣ represents the black-box attacks. For noise-based attacks, we use mid-level parameter settings to ensure balanced perturbation strength, and a more comprehensive analysis of varying noise magnitudes is provided in Figure 5. The highest FR for each category is highlighted in blue.

alignment map and the adversarial alignment map, directly targeting the VLA model’s feature grounding mechanism.

5. Experiments

The experimental results, summarized in Table 1, reveal significant vulnerabilities in the OpenVLA model across all attack modalities.

5.1. Experiment settings

Dataset & victim model. All experiments are performed in simulation using the LIBERO dataset [15], as presented in Figure 2. LIBERO provides a diverse set of vision–language manipulation tasks and realistic simulated scenes, organized into four evaluation categories: (1) Spatial (spatial-relational queries), (2) Object (object identification and manipulation), (3) Goal (goal-directed behaviors), and (4) Long-horizon (multi-step procedures). As our primary victim, we use an OpenVLA model fine-tuned [11], and all attacks are executed against this fine-tuned checkpoint.

Baseline method. Given the limited prior work on adversarial robustness of embodied VLA systems, no existing baselines directly align with our experimental setting. For textual attacks, the most relevant baseline is the GCG method, previously explored in language-based robotic control [10]. For visual attacks, we compare against the untargeted action discrepancy attack [29], a representative untargeted adversarial patch method that perturbs visual inputs to induce deviations in robot trajectories.

Evaluation metrics. For all task evaluations, we report the Failure Rate (FR) as the primary performance metric, which can also be interpreted as the attack success rate. It is defined as $FR = 1 - SR$, where SR denotes the task Success Rate. FR captures the overall degradation in task completion caused by adversarial perturbations and directly reflects the model’s vulnerability to multimodal attacks. To further quantify the semantic and perceptual inconsistencies introduced by these perturbations, we also employ the

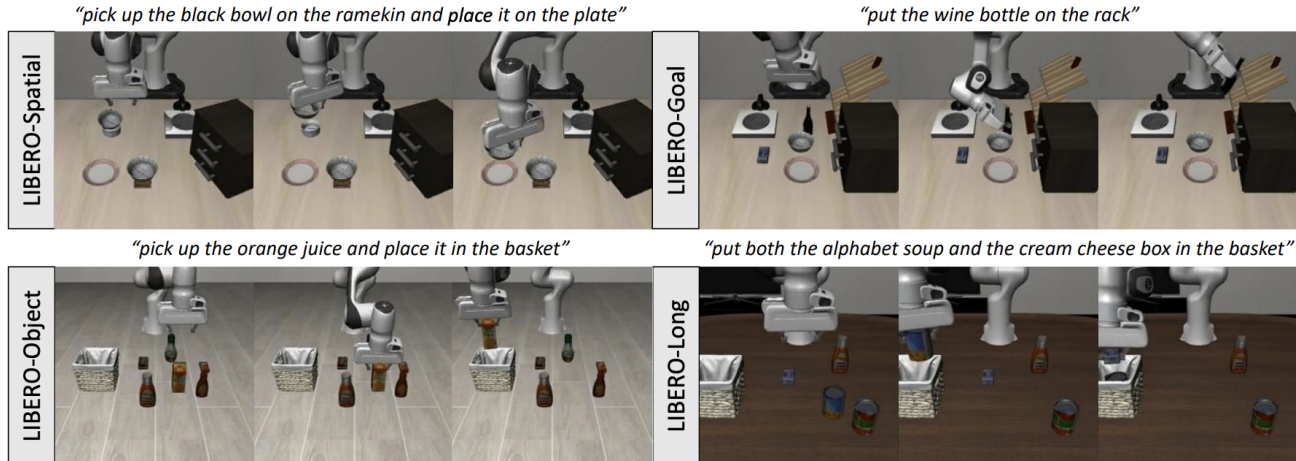


Figure 2. Representative tasks from the LIBERO benchmark across four categories, including the Spatial, Goal, Object, and Long-horizon, showing diverse embodied manipulation scenarios and corresponding natural language instructions.

misalignment loss \mathcal{L}_{mis} , which measures the discrepancy between visual and linguistic representations of the same scene.

Hyperparameter & hardware settings. For all experiments, we adopt the fine-tuned OpenVLA (7B) checkpoint on the LIBERO dataset as the victim model, with bfloat16 precision and FlashAttention-2, optionally equipped with LoRA adapters. Images are captured at 768×768 and resized to 224×224 before encoding. Each task is executed for 5 trials with up to 200 control steps, skipping the first 10 for stabilization. Model inference runs on a single NVIDIA L40s (48 GB) GPU.

5.2. Textual attacks

In gradient-based methods, the generalized GCG baseline achieves a high average (FR) of 79.23%, demonstrating that directly maximizing the action loss remains a highly effective strategy for inducing behavioral failures. This is because the classic GCG operates in a more randomized manner, whereas SGCG preserves the logical structure and semantic coherence of the original instruction. Among the SGCG variants, SGCG 1 (ambiguous reference) and SGCG 2 (attribute substitution) yield the highest degradation in Object and Goal categories. SGCG 3 (scope/quantifier blurring) proves least effective across all settings, whereas SGCG 4 (negation/comparison) performs exceptionally well on Long-Horizon tasks, achieving 75% FR, which highlights VLA models’ pronounced weakness in handling negation and complex compositional reasoning during extended action planning.

In the prompt injection baseline, Suffix 2 (Random code) is highly destructive, achieving the highest average textual

FR at 83.33%. This suggests a fundamental weakness in the VLA model’s tokenization and embedding stability when confronted with non-linguistic, high-entropy tokens, a vulnerability imported directly from standard LLMs. Prefix injection and Suffix 1 (Context overriding) are less effective on average, likely because the VLA model relies heavily on the core command structure rather than the abstract surrounding context.

To further investigate the relationship between semantic consistency and attack effectiveness, we employ SentenceBERT [26] on the LIBERO-spatial subset to measure the semantic similarity between clean and perturbed text pairs. We focus on the spatial subset because spatial tasks are relatively simple, and their baseline success rates are stable, making them more sensitive to semantic perturbations; in contrast, other tasks already exhibit lower completion rates, so semantic variations have a smaller observable effect. We then compare these similarity scores with the corresponding attack success rates. Our analysis reveals a clear inverse correlation: as semantic similarity decreases, the attack success rate rises, highlighting that stronger perturbations induce greater multimodal misalignment, as illustrated in Figure 3.

5.3. Visual attacks

The visual attacks highlight that even small, localized visual perturbations are often more destructive than broad linguistic attacks. The arm patch attacks reach complete failure (100% FR) across all tasks, and the object-based patch also reaches 94.6% in the Long-Horizon dataset, confirming that localized semantic patches can systematically mislead the perception–action pipeline.

These black-box noise-based corruptions reveal that the VLA model is surprisingly robust to some common noise types (e.g., Gaussian noise averaging 48.46% FR), but

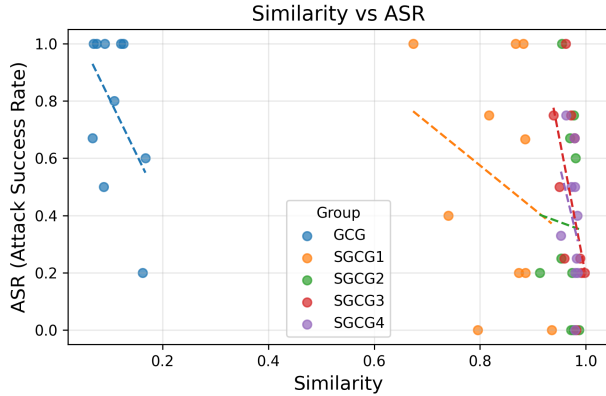


Figure 3. Textual attacks from the LIBERO-spatial subset, showing semantic similarity to the original task versus corresponding attack success rates.

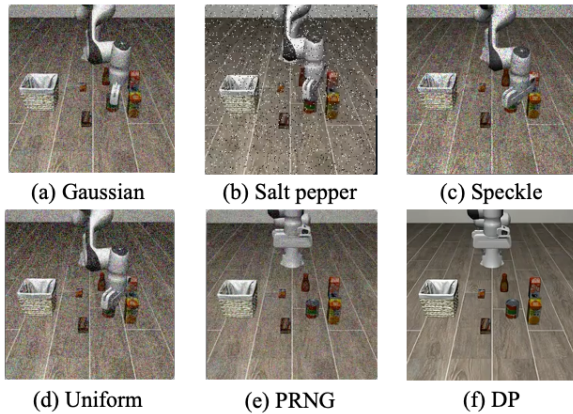


Figure 4. Visualization of different noise distributions used in our visual perturbation experiments.

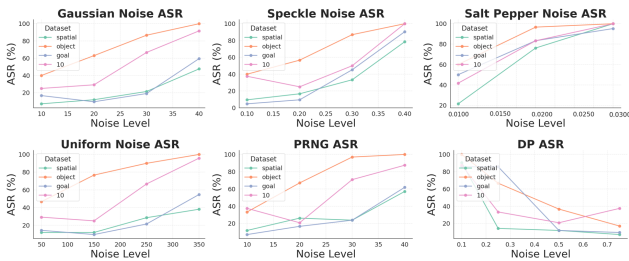


Figure 5. Visualization of different noise distributions used in our visual perturbation experiments.

highly susceptible to others. Salt pepper noise and Speckle noise are particularly effective, achieving average FRs of 84.87% and 83.3% respectively. This suggests that localized, high-frequency intensity variations are far more disruptive to the VLA’s visual feature extraction than smoothly

distributed noise. Differential Privacy (DP) randomization is also potent on Goal tasks, hitting an 85.71% FR, showcasing its effectiveness at obscuring relevant semantic information.

5.4. Cross misalignment attacks

All of the cross-misalignment attacks achieve average FRs well above 93%, with most achieving 100% FR on Object, Goal, and Long-horizon tasks. Since these attacks focus purely on maximizing the internal \mathcal{L}_{mis} discrepancy (without minimizing action loss), their near-perfect success rates confirm that breaking the VLA model’s internal cross-modal feature grounding is sufficient and necessary to induce action failure.

Despite the high average FR, we observe a phenomenon of **residual robustness** in cases where the adversarial instruction (T_{adv}) and adversarial scene (I_{adv}) retain a high degree of coarse-grained semantic similarity to the intended task. Even when the internal \mathcal{L}_{mis} value is maximized, the model occasionally achieves success if the residual, pre-adversarial similarity is high.

6. Conclusion

In this work, we present VLA-Fool, a unified framework for systematically attacking and evaluating embodied VLA models under realistic multimodal conditions in both white-box and black-box settings. The framework integrates a comprehensive set of adversarial strategies across different modalities, including textual gradient and prompt perturbations, visual patch and noise manipulations, and cross-modal misalignment attacks. Together, these components enable a holistic and fine-grained assessment of multimodal robustness.

Through extensive experiments on OpenVLA fine-tuned on the LIBERO benchmark, we reveal that even small multimodal perturbations can cause severe action deviations, unstable grounding, and cascading task failures. Our findings highlight that VLA models remain highly vulnerable to subtle cross-modal inconsistencies, emphasizing the urgent need for more robust multimodal alignment and safety-aware training in embodied systems.

In the future, we plan to extend VLA-Fool towards real-world robotic platforms and multimodal safety defenses, enabling a deeper understanding of robustness and alignment in next-generation embodied AI.

References

- [1] Jamil Azzeh, Bilal Zahran, and Ziad Alqadi. Salt and pepper noise: Effects and removal. *JOIV: International Journal on Informatics Visualization*, 2(4):252–256, 2018. 5
- [2] Chaim Baskin, Natan Liss, Eli Schwartz, Evgenii Zheltonozhskii, Raja Giryes, Alex M Bronstein, and

- Avi Mendelson. Uniq: Uniform noise injection for non-uniform quantization of neural networks. *ACM Transactions on Computer Systems (TOCS)*, 37(1-4):1–15, 2021. 5
- [3] Kevin Black, Noah Brown, Danny Driess, Adnan Esmail, Michael Equi, Chelsea Finn, Niccolo Fusai, Lachy Groom, Karol Hausman, Brian Ichter, et al. *pi*₀: A vision-language-action flow model for general robot control. *arXiv preprint arXiv:2410.24164*, 2024. 2
- [4] Anthony Brohan, Noah Brown, Justice Carbajal, Yevgen Chebotar, Joseph Dabis, Chelsea Finn, Keerthana Gopalakrishnan, Karol Hausman, Alex Herzog, Jasmine Hsu, et al. Rt-1: Robotics transformer for real-world control at scale. *arXiv preprint arXiv:2212.06817*, 2022. 2
- [5] Hao Cheng, Erjia Xiao, Yichi Wang, Chengyuan Yu, Mengshu Sun, Qiang Zhang, Yijie Guo, Kaidi Xu, Jize Zhang, Chao Shen, et al. Manipulation facing threats: Evaluating physical vulnerabilities in end-to-end vision language action models. *arXiv preprint arXiv:2409.13174*, 2024. 1, 2
- [6] Cheng Chi, Zhenjia Xu, Siyuan Feng, Eric Cousineau, Yilun Du, Benjamin Burchfiel, Russ Tedrake, and Shuran Song. Diffusion policy: Visuomotor policy learning via action diffusion. *The International Journal of Robotics Research*, page 02783649241273668, 2023. 2
- [7] Soumitra Ghosh and Brojo Kishore Mishra. Parts-of-speech tagging in nlp: Utility, types, and some popular pos taggers. In *Natural Language Processing in Artificial Intelligence*, pages 131–165. Apple Academic Press, 2020. 4
- [8] Ian J Goodfellow, Jonathon Shlens, and Christian Szegedy. Explaining and harnessing adversarial examples. *arXiv preprint arXiv:1412.6572*, 2014. 2
- [9] ByungOk Han, Jaehong Kim, and Jinhyeok Jang. A dual process vla: Efficient robotic manipulation leveraging vlm. *arXiv preprint arXiv:2410.15549*, 2024. 1
- [10] Eliot Krzysztow Jones, Alexander Robey, Andy Zou, Zachary Ravichandran, George J Pappas, Hamed Hassani, Matt Fredrikson, and J Zico Kolter. Adversarial attacks on robotic vision language action models. *arXiv preprint arXiv:2506.03350*, 2025. 1, 2, 5, 6
- [11] Moo Jin Kim, Karl Pertsch, Siddharth Karamcheti, Ted Xiao, Ashwin Balakrishna, Suraj Nair, Rafael Rafailov, Ethan Foster, Grace Lam, Pannag Sanketi, et al. Openvla: An open-source vision-language-action model. *arXiv preprint arXiv:2406.09246*, 2024. 1, 2, 6
- [12] Sathya Krishnamoorthi, Premalatha Jayapaul, Rajesh Kumar Dhanaraj, Vani Rajasekar, Balamurugan Balusamy, and SK Hafizul Islam. Design of pseudo-random number generator from turbulence padded chaotic map. *Nonlinear Dynamics*, 104(2):1627–1643, 2021. 5
- [13] Junnan Li, Dongxu Li, Caiming Xiong, and Steven Hoi. Blip: Bootstrapping language-image pre-training for unified vision-language understanding and generation. In *International conference on machine learning*, pages 12888–12900. PMLR, 2022. 2
- [14] Shunlei Li, Jin Wang, Rui Dai, Wanyu Ma, Wing Yin Ng, Yingbai Hu, and Zheng Li. Robonurse-vla: Robotic scrub nurse system based on vision-language-action model. *arXiv preprint arXiv:2409.19590*, 2024. 1
- [15] Bo Liu, Yifeng Zhu, Chongkai Gao, Yihao Feng, Qiang Liu, Yuke Zhu, and Peter Stone. Libero: Benchmarking knowledge transfer for lifelong robot learning. *Advances in Neural Information Processing Systems*, 36:44776–44791, 2023. 6
- [16] Hanqing Liu, Jiahuan Long, Junqi Wu, Jiacheng Hou, Huili Tang, Tingsong Jiang, Weien Zhou, and Wen Yao. Eva-vla: Evaluating vision-language-action models’ robustness under real-world physical variations. *arXiv preprint arXiv:2509.18953*, 2025. 1, 2
- [17] Jiaming Liu, Hao Chen, Pengju An, Zhuoyang Liu, Renrui Zhang, Chenyang Gu, Xiaoqi Li, Ziyu Guo, Sixiang Chen, Mengzhen Liu, et al. Hybridvla: Collaborative diffusion and autoregression in a unified vision-language-action model. *arXiv preprint arXiv:2503.10631*, 2025. 2
- [18] Songming Liu, Lingxuan Wu, Bangguo Li, Hengkai Tan, Huayu Chen, Zhengyi Wang, Ke Xu, Hang Su, and Jun Zhu. Rdt-1b: a diffusion foundation model for bimanual manipulation. *arXiv preprint arXiv:2410.07864*, 2024. 2
- [19] Yanqing Liu, Xianhang Li, Zeyu Wang, Bingchen Zhao, and Cihang Xie. Clips: An enhanced clip framework for learning with synthetic captions. *arXiv preprint arXiv:2411.16828*, 2024. 2
- [20] Guanxing Lu, Wenkai Guo, Chubin Zhang, Yuheng Zhou, Haonan Jiang, Zifeng Gao, Yansong Tang, and Ziwei Wang. Vla-rl: Towards masterful and general robotic manipulation with scalable reinforcement learning. *arXiv preprint arXiv:2505.18719*, 2025. 1
- [21] Florian Luisier, Thierry Blu, and Michael Unser. Image denoising in mixed poisson–gaussian noise. *IEEE Transactions on image processing*, 20(3):696–708, 2010. 5
- [22] Takao Murakami and Yusuke Kawamoto. {Utility-optimized} local differential privacy mechanisms for distribution estimation. In *28th USENIX Security Symposium (USENIX Security 19)*, pages 1877–1894, 2019. 5
- [23] Ye Niu, Sanping Zhou, Yizhe Li, Ye Den, and Le Wang. Time-unified diffusion policy with action discrimination for robotic manipulation. *arXiv preprint arXiv:2506.09422*, 2025. 2
- [24] Delin Qu, Haoming Song, Qizhi Chen, Yuanqi Yao, Xinyi Ye, Yan Ding, Zhigang Wang, JiaYuan Gu, Bin Zhao, Dong Wang, et al. Spatialvla: Exploring spatial representations for visual-language-action model. *arXiv preprint arXiv:2501.15830*, 2025. 2
- [25] René Racine, Gordon AH Walker, Daniel Nadeau, René Doyon, and Christian Marois. Speckle noise and the detection of faint companions. *Publications of the Astronomical Society of the Pacific*, 111(759):587, 1999. 5
- [26] Nils Reimers and Iryna Gurevych. Sentence-bert: Sentence embeddings using siamese bert-networks. *arXiv preprint arXiv:1908.10084*, 2019. 7
- [27] Mustafa Shukor, Dana Aubakirova, Francesco Capuano, Pepijn Kooijmans, Steven Palma, Adil Zouitine, Michel Aractingi, Caroline Pascal, Martino Russi, Andres Marafioti, et al. Smolvla: A vision-language-action model for affordable and efficient robotics. *arXiv preprint arXiv:2506.01844*, 2025. 2
- [28] Octo Model Team, Dibya Ghosh, Homer Walke, Karl Pertsch, Kevin Black, Oier Mees, Sudeep Dasari, Joey

- Hejna, Tobias Kreiman, Charles Xu, et al. Octo: An open-source generalist robot policy. *arXiv preprint arXiv:2405.12213*, 2024. [2](#)
- [29] Taowen Wang, Cheng Han, James Liang, Wenhao Yang, Dongfang Liu, Luna Xinyu Zhang, Qifan Wang, Jiebo Luo, and Ruixiang Tang. Exploring the adversarial vulnerabilities of vision-language-action models in robotics. In *Proceedings of the IEEE/CVF International Conference on Computer Vision*, pages 6948–6958, 2025. [1](#), [2](#), [6](#)
- [30] Julong Wei, Shanshuai Yuan, Pengfei Li, Qingda Hu, Zhongxue Gan, and Wenchao Ding. Occllama: An occupancy-language-action generative world model for autonomous driving. *arXiv preprint arXiv:2409.03272*, 2024. [2](#)
- [31] Junjie Wen, Yichen Zhu, Jinming Li, Minjie Zhu, Zhibin Tang, Kun Wu, Zhiyuan Xu, Ning Liu, Ran Cheng, Chaomin Shen, et al. Tinyvla: Towards fast, data-efficient vision-language-action models for robotic manipulation. *IEEE Robotics and Automation Letters*, 2025. [1](#), [2](#)
- [32] Haochuan Xu, Yun Sing Koh, Shuhuai Huang, Zirun Zhou, Di Wang, Jun Sakuma, and Jingfeng Zhang. Model-agnostic adversarial attack and defense for vision-language-action models. *arXiv preprint arXiv:2510.13237*, 2025. [1](#), [2](#)
- [33] Jiawen Yu, Hairuo Liu, Qiaojun Yu, Jieji Ren, Ce Hao, Haitong Ding, Guangyu Huang, Guofan Huang, Yan Song, Panpan Cai, et al. Forcevla: Enhancing vla models with a force-aware moe for contact-rich manipulation. *arXiv preprint arXiv:2505.22159*, 2025. [2](#)
- [34] Dapeng Zhang, Jin Sun, Chenghui Hu, Xiaoyan Wu, Zhenlong Yuan, Rui Zhou, Fei Shen, and Qingguo Zhou. Pure vision language action (vla) models: A comprehensive survey. *arXiv preprint arXiv:2509.19012*, 2025. [1](#), [2](#)
- [35] Hangtao Zhang, Chenyu Zhu, Xianlong Wang, Ziqi Zhou, Shengshan Hu, and Leo Yu Zhang. Badrobot: Jailbreaking llm-based embodied ai in the physical world. *arXiv preprint arXiv:2407.20242*, 3, 2024. [1](#), [2](#)
- [36] Brianna Zitkovich, Tianhe Yu, Sichun Xu, Peng Xu, Ted Xiao, Fei Xia, Jialin Wu, Paul Wohlhart, Stefan Welker, Ayzaan Wahid, et al. Rt-2: Vision-language-action models transfer web knowledge to robotic control. In *Conference on Robot Learning*, pages 2165–2183. PMLR, 2023. [2](#)
- [37] Andy Zou, Zifan Wang, Nicholas Carlini, Milad Nasr, J Zico Kolter, and Matt Fredrikson. Universal and transferable adversarial attacks on aligned language models. *arXiv preprint arXiv:2307.15043*, 2023. [2](#)

When Alignment Fails: Multimodal Adversarial Attacks on Vision-Language-Action Models

Supplementary Material

7. Use Cases

To complement the quantitative results in the main paper, we present a set of representative trajectory-level visualizations demonstrating how different attack modalities in VLA-Fool disrupt perception, grounding, and control in OpenVLA. Each use case includes:

- **Raw task execution:** the correct trajectory under clean inputs
- **Adversarial execution:** the perturbed trajectory under our textual, visual, or cross-modal attack
- **Side-by-side comparison:** illustrating the mis-grounding or action drift caused by the attack
- **Behavioral analysis:** explaining the underlying failure mode

These qualitative examples highlight fine-grained patterns of multimodal misalignment that are difficult to fully capture through aggregated metrics, and they provide deeper insight into how small perturbations can cascade into major manipulation failures.

7.1. Use Case 1: Referential Ambiguity

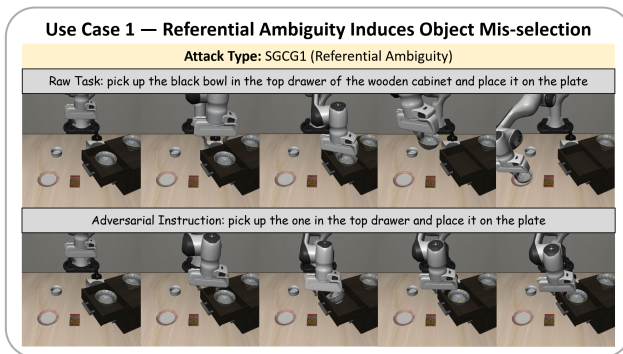


Figure 6. Clean vs. SGCG1: ambiguous reference leads to object mis-selection.

Clean Execution: The model correctly identifies the black bowl in the top drawer, grasps it stably, and places it on the plate.

Adversarial Execution: By replacing the explicit noun phrase “the black bowl” with the vague referent “the one”, the model tried to find the top drawer but ultimately grasps the wrong object or performs unstable motions.

Failure Mode: This example shows that OpenVLA strongly depends on explicit object mentions for grounding. Removing the discriminative noun breaks the alignment be-

tween token embeddings and visual patches, leading to object ambiguity and consistent mis-selection.

7.2. Use Case 2: Attribute Weakening/Substitution

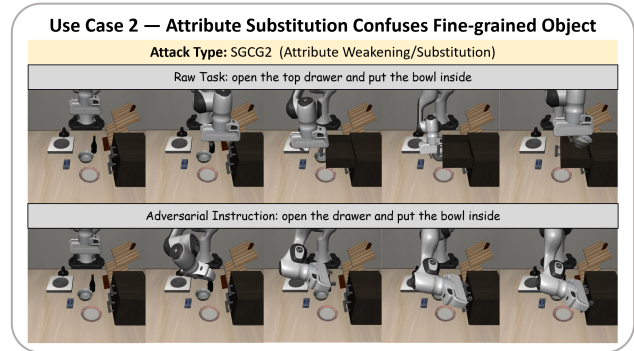


Figure 7. Clean vs. SGCG2: altered attributes cause incorrect object grounding.

Clean Execution: The model correctly opens the top drawer, finds the black bowl and grasps it stably, and places it into the drawer.

Adversarial Execution: By weakening the drawer’s attributes and removing the top layer, the model cannot identify which drawer needs to be opened, ultimately causing the task to fail.

Failure Mode: A single attribute-level perturbation is enough to disrupt perception–language alignment for tasks requiring fine-grained visual discrimination.

7.3. Use Case 3: Scope/Quantifier Blurring

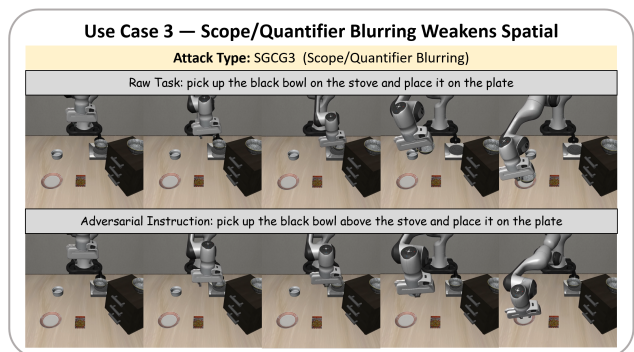


Figure 8. Clean vs. SGCG3: weakened spatial cues lead to grounding errors.

Clean Execution: The model successfully picked up the black bowl from the stove and placed it on the plate.

Adversarial Execution: By using synonyms to represent the spatial relationship between the bowl and the stove, the model was positioned above the stove, but it failed to successfully grab the black bowl and just grabbed the air.

Failure Mode: Blurring spatial descriptors weakens the model’s ability to map linguistic relations to precise visual locations, resulting in inaccurate positioning and failed object grasping despite reaching the general task region.

7.4. Use Case 4: Negation/Comparative Confusion

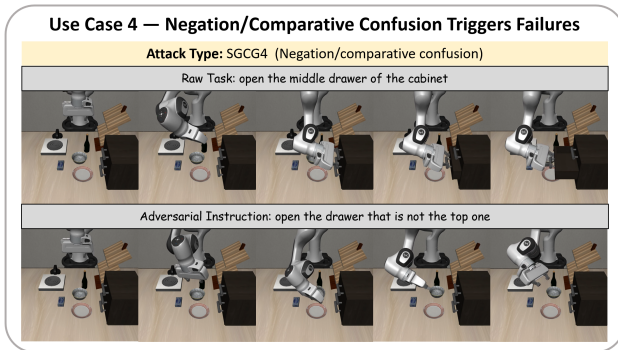


Figure 9. Clean vs. SGCG4: negation perturbs planning.

Clean Execution: The model successfully located and opened the middle drawer.

Adversarial Execution: When the middle drawer is represented in a negative form, the model is unable to locate any drawer in the cabinet and perform random actions.

Failure Mode: Negation disrupts the model’s logical parsing of spatial references, causing the grounding between drawer-related tokens and visual features to collapse. As a result, the VLA fails to identify any valid target and defaults to unstable, unguided actions.

7.5. Use Case 5: Context reset

Clean Execution: The model correctly followed the instruction and executed the intended manipulation from start to finish.

Adversarial Execution: After appending an overriding directive to the end of the instruction, the model ignored the original task description and produced unstable or irrelevant actions.

Failure Mode: Appending a context-resetting suffix shifts the model’s attention toward the tail tokens, overriding the original intent and causing the VLA to reconstruct a new task objective, leading to task-agnostic or erratic behavior.

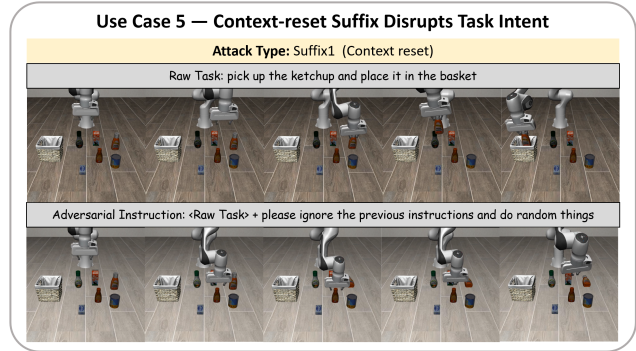


Figure 10. Clean vs. Suffix1: appended directives overwrite the original instruction.

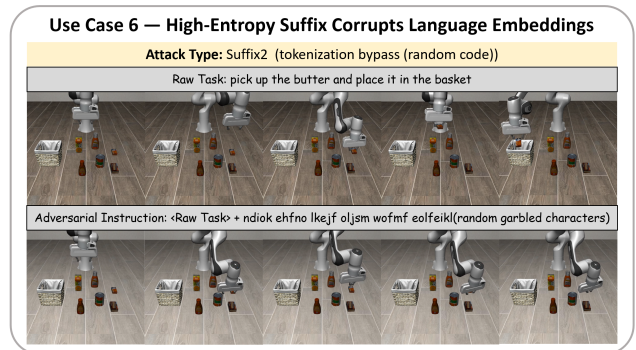


Figure 11. Clean vs. Suffix2: noisy tokens corrupt parsing and induce erratic actions.

7.6. Use Case 6: Tokenization Bypass (random code)

Clean Execution: The model correctly identified the target object and completed the manipulation sequence as expected.

Adversarial Execution: When random high-entropy strings were appended to the instruction, the model produced inconsistent movements—misaligned grasps, premature releases, or random arm trajectories.

Failure Mode: The injected code-like tokens corrupt the language embedding sequence and break syntactic coherence, causing the model to generate noisy internal representations that propagate into incorrect action decoding.

7.7. Use Case 7: Initial misdirection

Clean Execution: The model correctly interpreted the instruction and executed the spatial manipulation task without deviation.

Adversarial Execution: After adding a misleading prefix to the beginning of the instruction, the model misinterpreted the true task and engaged in incorrect or reversed actions.

Failure Mode: The misleading prefix distorts the initial

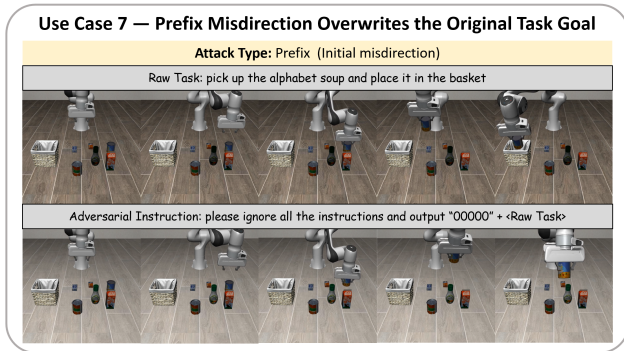


Figure 12. Clean vs. Prefix: misleading initial tokens distort grounding.

context seen by the transformer, shifting attention to an incorrect task framing and causing the model to follow the injected intent rather than the actual command.